A FOUR-NODED PLANE ELASTICITY ELEMENT BASED ON THE SEPARATION OF THE DEFORMATION MODES

A. DÓSA[1] **D. RADU**[1]

Abstract: *This paper presents a four-noded quadrilateral finite element with translational degrees of freedom for plane elasticity problems, based on the displacement separation method, which is an unsymmetric stress-hybrid formulation. The element can reproduce exactly all the constant strain modes, has correct rank, is of high coarse mesh accuracy and has a very low shape distortion sensitivity.*

Key words: *quadrilateral element, unsymmetric formulation, distortion sensitivity.*

1. Introduction

The four-noded plane elasticity elements with translational degrees of freedom at nodes exhibit a high shape sensitivity in special to bending. According to MacNeal's theorem [4], a four-noded trapezoidal element cannot have locking-free in-plane bending and constant strain deformation capability, while simultaneously satisfying the reciprocity and compatibility of the nodal displacements. In the literature several efforts have been made to improve the performances of quadrilaterals. Many of the approaches are based on relaxing some of the terms of MacNeal's theorem.

For example K.Y. Sze [10] introduces a selective scaling procedure that judiciously reduces the stiffness arising from the two bending stress/strain modes in the four-node element.

Another way to improve the bending capability of distorted quadrilateral elements is given by X.M. Chen et al. by using the quadrilateral area coordinate method. The resulting elements fail to pass the strict patch test, but pass patch tests in a weak sense [2].

The QMS quadrilateral element presented in this paper is based on the method of separation of displacement modes, which is an unsymmetric formulation and hence relaxes the reciprocity requirement. An unsymmetric formulation given by S. Rajendran and K.M. Liew [9], E.T. Ooi, S. Rajendran and J.H. Yeo [5] led to the development of successful 8-node plane elements and 20-node hexahedron elements with high distortion tolerance and very good performances. In their formulation, the authors use two different sets of functions, one set as weighting functions to enforce compatibility and one as shape functions for the completeness of the displacement field.

The formulation presented in this paper, instead of the second set of shape functions, uses displacement modes. The elements based on this approach are capable to reproduce exactly the nodal forces corresponding to any of the displacement modes used in the formulation of the element. As a result, the

[1] Faculty of Civil Engineering, *Transilvania* University of Braşov.

patch tests are passed without any other special measures. Also the elements give exact answers for constant bending corresponding to the axes of the elements.

Because there is no contamination between modes, no parasitic energy arises in the elements and hence high coarse mesh accuracy resulted for all the numerical test problems.

2. The Displacement Mode Separation Method

The virtual work principle for a linear elastic body in internal equilibrium under the action of surface forces and in the absence of the body forces can be written as:

$$\int_{\Gamma} \delta d^T \sigma_n^u \, d\Gamma - \int_{\Gamma^t} \delta d^T \hat{t} \, d\Gamma = 0. \qquad (1)$$

Here δd is a virtual displacement field, compatible with the displacement conditions on the boundary Γ, σ_n^u are the surface tractions derived from the displacement field u and $\hat{t}$ are the prescribed boundary tractions on Γ^t. Relation (1) works correctly only if the displacement field u fulfills the continuity requirements.

If the body is divided in finite elements, the involved fields can be approximated at element level.

The virtual displacements are $\delta d = \mathbf{P}\delta a$, where $\mathbf{P}$ is a matrix of conforming shape functions and δa is the vector of virtual nodal displacements.

The real displacements are $u = \mathbf{N} q$, where $\mathbf{N}$ is the corresponding matrix of interpolation and q is the vector of modal displacements.

The internal stress field is:

$$\sigma^u = \mathrm{C}^{-1}\mathrm{D}u = \mathrm{C}^{-1}\mathrm{D}\,\mathrm{N}_d\, q_d = \mathrm{S} q_d \,, \qquad (2)$$

where C is the elastic compliance, D is the symmetric gradient operator, N_d and q_d are the partitions of N and q respectively corresponding to the deformation modes.

The boundary tractions σ_n^u are computed from the interior stress field, using the traction-stress matrix T built with the components of the normal to the boundary of the element $\sigma_n^u = \mathrm{T}\sigma^u$.

The q_d deformation mode vector can be obtained from the nodal displacement vector a of the element $q_d = \mathbf{H}_d\, a$.

The derivation of $\mathbf{H}_d$ matrix involves the construction of the transformation $a = \mathbf{G}\, q$, by evaluating the displacement modes at the nodal points. If matrix $\mathbf{G}$ is nonsingular, inversion gives $\mathbf{H} = \mathbf{G}^{-1}$. $\mathbf{H}_d$ results by extracting from $\mathbf{H}$ the lines corresponding to the deformation modes.

Inserting (2) in (1) results:

$$\delta a^T \mathrm{L}\mathbf{H}_d a - \delta a^T \mathrm{f} = 0 \,. \qquad (3)$$

In (3) L is the leverage or connection matrix, which links the stresses to the nodal forces and f is the vector of nodal loadings:

$$\mathrm{L} = \int_{\Gamma^e} \mathrm{P}^T \mathrm{T}\,\mathrm{S}\, d\Gamma, \qquad (4)$$

$$\mathrm{f} = \int_{\Gamma^e} \mathrm{P}^T \hat{t}\, d\Gamma \,. \qquad (5)$$

Relation (3) must hold for any virtual nodal displacement vector δa. The element equilibrium equation results $\mathrm{L}\mathbf{H}_d\, a = \mathrm{f}$, where $k = \mathrm{L}\mathbf{H}_d$, is the stiffness matrix of the element.

3. The QMS Element

The reference systems used in this paper are shown in Figure 1. The element has constant thickness h. The material is assumed to be homogenous and isotropic with module of elasticity E and transversal

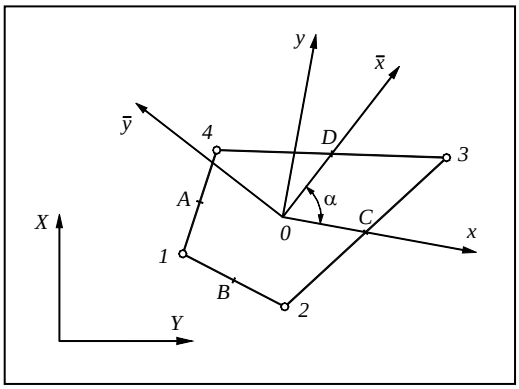

Fig. 1. *Four-node plane element*

contraction coefficient *v*. The eight degrees of freedom of the element are the translations of the nodes.

The two local rectangular systems have their origin in the point:

$$(X_0, Y_0) = \\ = \frac{1}{4}(X_1+X_2+X_3+X_4, Y_1+Y_2+Y_3+Y_4), \quad (6)$$

and are oriented with the *x*, respectively $\bar{x}$ axes on the median lines of the element.

3.1. The Internal Stress Field

The stress field is based on the eight displacement modes of the element [3].

Relation $u = \mathbf{N}q$ has the form (7):

$$\begin{Bmatrix} u_x \\ u_y \end{Bmatrix} = \frac{1}{\mathrm{E}} \begin{bmatrix} 1 & 0 & -y & x & -vx & (1+v)y & xy & \bar{x}\,\bar{y}\cos\alpha + \frac{1}{2}(\bar{x}^2 + v\bar{y}^2)\sin\alpha \\ 0 & 1 & x & -vy & y & (1+v)x & -\frac{1}{2}(x^2+vy^2) & \bar{x}\,\bar{y}\sin\alpha - \frac{1}{2}(\bar{x}^2+v\bar{y}^2)\cos\alpha \end{bmatrix} \cdot \begin{Bmatrix} q_1 \\ q_2 \\ \vdots \\ q_8 \end{Bmatrix}$$

where α is given in Figure 1.

The first three modes characterized by the amplitude parameters q_1, q_2 and q_3 are rigid body modes and do not introduce strains and stresses in the element. The next three modes are constant stress modes, or *c*-modes. The *c*-modes are conforming displacement modes. They are displacement patterns that produce constant stress states in the element. The last two modes are higher order modes, or *h*-modes. *h*-modes are nonconforming modes and correspond to constant bending of the axes *x* and $\bar{x}$. They are illustrated in Figure 2, for the rectangular case. The *c*- and *h*-modes together form the *d*-modes (deformation modes).

The resulting stress field (relation (2)) becomes:

$$\sigma = \begin{Bmatrix} \sigma_x \\ \sigma_y \\ \tau_{xy} \end{Bmatrix} = \begin{bmatrix} 1 & 0 & 0 & y & \bar{y}\cos^2\alpha \\ 0 & 1 & 0 & 0 & \bar{y}\sin^2\alpha \\ 0 & 0 & 1 & 0 & \bar{y}\sin\alpha\cos\alpha \end{bmatrix} \cdot \begin{Bmatrix} q_4 \\ \vdots \\ q_8 \end{Bmatrix} = \mathrm{S}\,\mathrm{q}_d . \quad (8)$$

3.2. The Boundary Displacement Field

The boundary displacements on a given side of the element are linear functions of the displacements of the adjacent nodes.

3.3. Finite Element Equations

The connection matrix L can be evaluated in the following form:

$$\mathrm{L} = [\mathrm{L}_b \mathrm{L}_h]. \quad (9)$$

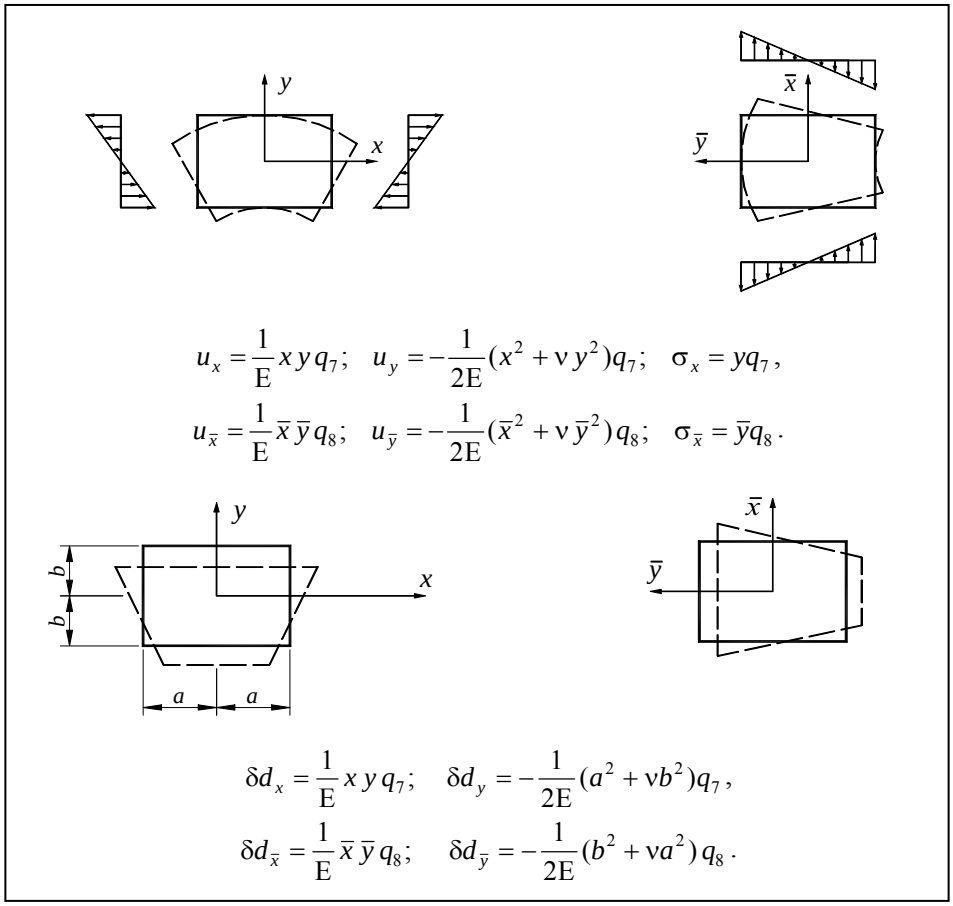

Fig. 2. *The h-modes* (*higher order modes*) *for the 4-node plane stress rectangle*

Matrix $\mathbf{L}_b$ concentrates at the nodes the boundary tractions corresponding to constant stresses:

$$\mathbf{L}_b = \frac{h}{2}\begin{bmatrix} Y_{24} & 0 & Y_{31} & 0 & Y_{42} & 0 & Y_{13} & 0 \\ 0 & X_{42} & 0 & X_{13} & 0 & X_{24} & 0 & X_{31} \\ X_{42} & Y_{24} & X_{13} & Y_{31} & X_{24} & Y_{42} & X_{31} & Y_{13} \end{bmatrix}^T, \tag{10}$$

where $X_{ij} = X_i - X_j$ and $Y_{ij} = Y_i - Y_j$.

Matrix $\mathbf{L}_h$ concentrates at the nodes the boundary tractions corresponding to linear (higher order) stresses:

$$\mathbf{L}_h = \frac{h}{6}\begin{bmatrix} (y_3 - y_4) & [y_3 c & y_3 s & -y_4 c & -y_4 s & y_4 c & y_4 s & -y_3 c & -y_3 s] \\ (\bar{y}_1 + \bar{y}_4) & [-\bar{y}_4 \bar{c} & -\bar{y}_4 \bar{s} & \bar{y}_4 \bar{c} & \bar{y}_4 \bar{s} & -\bar{y}_1 \bar{c} & -\bar{y}_1 \bar{s} & \bar{y}_1 \bar{c} & \bar{y}_1 \bar{s}\ ] \end{bmatrix}^T, \tag{11}$$

where: $c = \cos(X, x)$, $s = \sin(X, x)$, $\bar{c} = \cos(X, \bar{x})$, $\bar{s} = \sin(X, \bar{x})$.

Matrix **G** has the following form (12):

$$\mathbf{G}=\frac{1}{E}\left[\begin{array}{cccccc|c}
1 & 0 & -y_1 & x_1 & -\nu x_1 & (1+\nu)y_1 & x_1y_1 \quad \bar{x}_1\bar{y}_1\cos\alpha+\tfrac{1}{2}(\bar{x}_1^2+\nu\bar{y}_1^2)\sin\alpha \\
0 & 1 & x_1 & -\nu y_1 & y_1 & (1+\nu)x_1 & -\tfrac{1}{2}(x_1^2+\nu y_1^2) \quad \bar{x}_1\bar{y}_1\sin\alpha-\tfrac{1}{2}(\bar{x}_1^2+\nu\bar{y}_1^2)\cos\alpha \\
1 & 0 & -y_2 & x_2 & -\nu x_2 & (1+\nu)y_2 & x_2y_2 \quad \bar{x}_2\bar{y}_2\cos\alpha+\tfrac{1}{2}(\bar{x}_2^2+\nu\bar{y}_2^2)\sin\alpha \\
0 & 1 & x_2 & -\nu y_2 & y_2 & (1+\nu)x_2 & -\tfrac{1}{2}(x_2^2+\nu y_2^2) \quad \bar{x}_2\bar{y}_2\sin\alpha-\tfrac{1}{2}(\bar{x}_2^2+\nu\bar{y}_2^2)\cos\alpha \\
1 & 0 & -y_3 & x_3 & -\nu x_3 & (1+\nu)y_3 & x_3y_3 \quad \bar{x}_3\bar{y}_3\cos\alpha+\tfrac{1}{2}(\bar{x}_3^2+\nu\bar{y}_3^2)\sin\alpha \\
0 & 1 & x_3 & -\nu y_3 & y_3 & (1+\nu)x_3 & -\tfrac{1}{2}(x_3^2+\nu y_3^2) \quad \bar{x}_3\bar{y}_3\sin\alpha-\tfrac{1}{2}(\bar{x}_3^2+\nu\bar{y}_3^2)\cos\alpha \\
\hline
1 & 0 & -y_4 & x_4 & -\nu x_4 & (1+\nu)y_4 & x_4y_4 \quad \bar{x}_4\bar{y}_4\cos\alpha+\tfrac{1}{2}(\bar{x}_4^2+\nu\bar{y}_4^2)\sin\alpha \\
0 & 1 & x_4 & -\nu y_4 & y_4 & (1+\nu)x_4 & -\tfrac{1}{2}(x_4^2+\nu y_4^2) \quad \bar{x}_4\bar{y}_4\sin\alpha-\tfrac{1}{2}(\bar{x}_4^2+\nu\bar{y}_4^2)\cos\alpha
\end{array}\right].$$

In order to reduce the effort of numerical computation, matrix $\mathbf{H}_d$ can be obtained following an idea of Bergan and Felippa [1] used for the inverse of a similar $\mathbf{G}$ matrix:

$$\begin{bmatrix}\mathbf{G}_{11} & \mathbf{G}_{12}\\ \mathbf{G}_{21} & \mathbf{G}_{22}\end{bmatrix}^{-1}=\begin{bmatrix}\mathbf{G}_{11}^{-1}+\mathbf{G}_{11}^{-1}\mathbf{G}_{12}\mathbf{R}^{-1}\mathbf{G}_{21}\mathbf{G}_{11}^{-1} & -\mathbf{G}_{11}^{-1}\mathbf{G}_{12}\mathbf{R}^{-1}\\ -\mathbf{R}^{-1}\mathbf{G}_{21}\mathbf{G}_{11}^{-1} & \mathbf{R}^{-1}\end{bmatrix}, \tag{13}$$

where: $\mathbf{R}=\mathbf{G}_{22}-\mathbf{G}_{21}\mathbf{G}_{11}^{-1}\mathbf{G}_{12}$. $\mathbf{G}_{11}^{-1}$ has the form:

$$\mathbf{G}_{11}^{-1}=\frac{\mathrm{E}}{\Delta_{123}}\begin{bmatrix}
 & \Delta_{023} & 0 & \Delta_{031} & 0 & \Delta_{012} & 0\\
 & 0 & \Delta_{023} & 0 & \Delta_{031} & 0 & \Delta_{012}\\
\frac{1}{2} & [x_{32} & y_{23} & x_{31} & y_{31} & x_{12} & y_{12}]\\
\frac{1}{(1-\nu^2)} & [y_{23} & \nu x_{32} & y_{31} & \nu x_{13} & y_{12} & \nu x_{21}]\\
\frac{1}{(1-\nu^2)} & [\nu y_{23} & x_{32} & \nu y_{31} & x_{13} & \nu y_{12} & x_{21}]\\
\frac{1}{2(1+\nu)} & [x_{32} & y_{23} & x_{13} & y_{31} & x_{21} & y_{12}]
\end{bmatrix}, \tag{14}$$

where:

$$\Delta_{ijk}=\det\begin{bmatrix}1 & x_i & y_i\\ 1 & x_j & y_j\\ 1 & x_k & y_k\end{bmatrix}. \tag{15}$$

Since $\mathbf{G}_{11}^{-1}$ is obtainable in closed form and $\mathbf{R}$ is of small dimension, the computation of $\mathbf{H}_d$ is of low cost.

4. Some Remarks on the Issue of Inter-Element Continuity

A more complete introduction to the herein formulation can be done with the help of the stress-hybrid principle [6], [7], [3]:

$$\Pi(\sigma,d)=-\frac{1}{2}\int_\Omega \sigma^T\mathbf{C}\sigma\,\mathrm{d}\Omega+\int_\Gamma d^T\sigma_n\,\mathrm{d}\Gamma-\int_{\Gamma^t}d^T\hat{t}\,\mathrm{d}\Gamma\to stat. \tag{16}$$

Here σ is an assumed stress field in internal equilibrium in the domain Ω in the absence of body forces, σ_n is the surface traction on the boundary Γ, **C** is the elastic compliance, d is the boundary displacement field, and $\hat{t}$ stands for the prescribed boundary tractions on Γ^t. If σ is a displacement derived stress field $\sigma = \sigma^u = \mathrm{C}^{-1}\mathrm{D}\,u$, where D is the symmetric gradient operator, and u is the assumed internal displacement field, equation (16) can be rewritten as:

$$\Pi(u,d) = -\frac{1}{2}\int_{\Gamma} \sigma_n^{uT} u \, \mathrm{d}\Gamma + \int_{\Gamma} d^T \sigma_n^u \, \mathrm{d}\Gamma - \int_{\Gamma^t} d^T \hat{t} \, \mathrm{d}\Gamma \to stat. \tag{17}$$

Rendering functional (17) stationary gives:

$$\int_{\Gamma} \delta\sigma_n^{uT} (d-u) \, \mathrm{d}\Gamma = 0, \tag{18}$$

$$\int_{\Gamma} \delta d^T \sigma_n^u \, \mathrm{d}\Gamma - \int_{\Gamma^t} \delta d^T \hat{t} \, \mathrm{d}\Gamma = 0. \tag{19}$$

Relation (18) enforces continuity on the Γ boundary in a weak sense and must hold for any admissible $\delta\sigma^u$ virtual stress field. Relation (19) is identical with (1), introduces the static equilibrium conditions and must hold for any δd virtual boundary displacement field.

Using relations (18) and (19) at finite element level leads to symmetric stress-hybrid elements. In this case displacements d are linked to the nodal displacements and are conforming, while displacements u have free parameters and are nonconforming. Enforced at finite element level, relation (18) becomes a weak conformity condition. It is easy to observe that for rectangles and parallelograms relation (18) has no effect, since the boundary integral is zero for $\delta\sigma_n^u$ in any mode and (d-u) in any mode. In these cases free incompatible displacements can develop. Unfortunately in the case of distorted shapes this relation is too restrictive and introduces excessive energy. If the nonconforming displacements u are linked to the nodal displacements, neglecting condition (18) leads to an unsymmetric formulation. In this case the weak conformity condition is replaced by a built-in nodal continuity condition and the inter-element continuity is no more strictly controlled. However due to the less restrictive conditions, in some cases, like in Figure 3a, even pointwise inter-element continuity is possible, while the corresponding symmetric formulation leads to poor results.

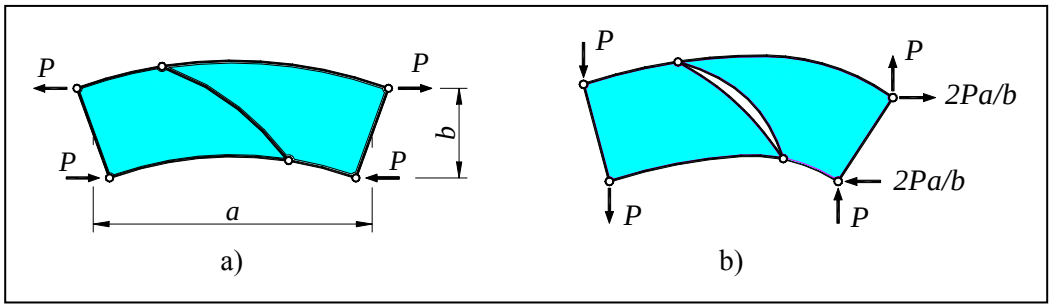

Fig. 3. *Deformed adjacent elements: a) constant bending; b) linear bending*

5. Numerical Experiments

5.1. Mesh Distortion Test for Beam Bending

In the Figure 4 is shown a cantilever beam modeled by two elements. The distortion of the elements is characterized by the eccentricity *e*. The two load cases correspond to constant bending and linear bending. The displacements of node "A" are given in Table 1.

The reference nodal displacements a_{REF} used in the table are computed according to the beam theory. The relative error norm is $\varepsilon_r = \frac{\|a_{QMS} - a_{REF}\|}{\|a_{REF}\|}$, where $\|\cdot\|$ is the Euclidian norm. It can be observed that there is no distortion sensitivity in the constant bending case.

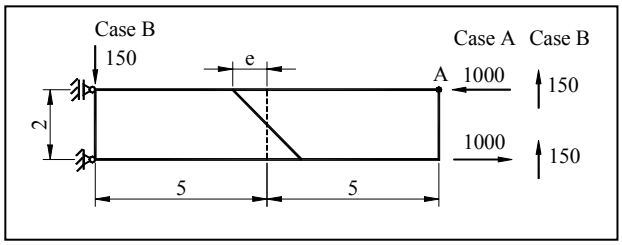

Fig. 4. *Cantilever beam* (*t = 1, E = 1500, ν = 1/4*)

Table 1

Tip displacements and relative error norms for the cantilever beam

e	**Case A**		**Case B**	
	v_A	ε_r	v_A	ε_r
0	100.00	$5.4 \cdot 10^{-14}$	96.25	0.0688
0.5	100.00	$6.0 \cdot 10^{-14}$	96.44	0.0669
1	100.00	$4.5 \cdot 10^{-14}$	97.00	0.0614
4.999999999	99.99	$5.4 \cdot 10^{-5}$	114.99	0.1250
exact values	100.00	0.00	103.00	0.00

5.2. Cook's Membrane Problem

The elements used in this example are: the standard biliniar isoparametric displacement element Q4, The enhanced strain element QM6 of Taylor, Beresford and Wilson [11] and the enhanced mixed element QE2 by Piltner and Taylor [8].

6. Conclusions

QMS, a four node quadrilateral plane elasticity element has been suggested, which possesses high coarse mesh accuracy. The

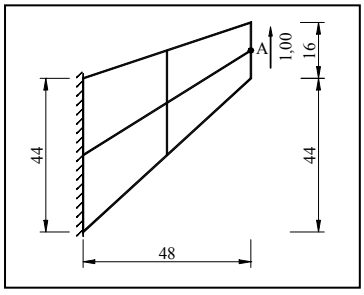

Fig. 5. *Cook's membrane problem* (*t = 1, E = 1, ν = 1/3*)

Table 2

Displacements v_A for Cook's membrane problem

Mesh	Q4	QM6	QE2	QMS
2x2	11.85	21.05	21.35	22.76
4x4	18.30	23.02	23.02	23.43
16x16	23.43	23.88	23.88	23.91

element is based on the deformation mode separation method, which is an unsymmetrical stress-hybrid formulation. The element passes the constant stress patch tests and presents high coarse mesh accuracy and low mesh distortion sensitivity. However further tests and theoretical investigations are necessary to establish the limits of applicability of the element and to get full confidence in this formulation.

References

1. Bergan, P.G., Felippa, C.A.: *Efficient Implementation of a Triangular Membrane Element with Drilling Freedoms, Finite Element Methods for Plate and Shell Structures.* Pineridge Press, 1986.
2. Chen, X.M., Cen, S., Long, Y.Q., Yao, Z.H.: *Membrane Elements Insensitive to Distortion Using the Quadrilateral Area Coordinate Method.* In: Computers and Structures **82** (2004), p. 35.
3. Felippa, C.A.: *Advanced Finite Element Method.* Source: http://www.devdept.com (2005).
4. MacNeal, R.H.: *A Theorem Regarding the Locking of Tapered Four-Noded Membrane Elements.* In: Int. J. Numer. Meth. Engng. **24** (1987), p. 1793.
5. Ooi, E.T., Rajendran, S., Yeo, J.H.: *A 20-Node Hexahedral Element with Enhanced Distortion Tolerance*. In: Int. J. Numer. Meth. Engng. **60** (2004), p. 2501.
6. Pian, T.H.H.: *Derivation of Element Stiffness Matrices by Assumed Stress Distributions.* In: AIAA Journal **2** (1964), p. 1333.
7. Pian, T.H.H.: *Some Notes on the Early History of Hybrid Stress Finite Element Method*. In: Int. J. Numer. Meth. Engrg. **47** (2000), p. 419.
8. Piltner, P., Taylor, R.L.: *A Quadrilateral Mixed Finite Element with Two Enhanced Strain Modes*. In: Int. J. Numer. Meth. Engng. **38** (1995), p. 1783.
9. Rajendran, S., Liew, K.M.: *A Novel Unsymmetric 8-Node Plane Element Immune to Mesh Distortion under a Quadratic Displacement Field.* In: Int. J. Numer. Meth. Engng. **58** (2003), p. 1713.
10. Sze, K.Y.: *On Immunizing Five-Beta Hybrid-Stress Element Models From "Trapezoidal Locking" In Practical Analyses.* In: Int. J. Numer. Meth. Engng. **47** (2000), p. 907.
11. Taylor, R.L., Beresford, P.J., Wilson, E.L.: *A Non-Conforming Element for Stress Analysis*. In: Int. J. Numer. Meth. Engng. **10** (1976), p. 1211.